「Macromolecular Research」 목차

정기간행영문지_ 27권 11호 · 2019년 11월

COVER PAPER

Preparation of Degradable Polymeric Nanoparticles with Various Sizes and Surface Charges from Polycarbonate Block Copolymers

Gyu Seong Heo, Sangho Cho*, and Karen L. Wooley*

Vol. 27, No. 11, pp 1173-1178 (2019) | NOV 25, 2019 | DOI 10.1007/s13233-020-8044-x

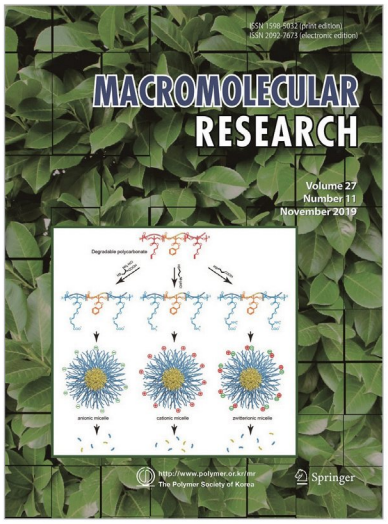

Degradable polycarbonate-based ABA-type block copolymers with pendant vinyl ether and benzyl ester functionalities were synthesized by organocatalytic sequential ring-opening polymerization of functional cyclic carbonate monomers. The vinyl ether moieties on the resultingblock copolymers were readily conjugated with differently charged thiol compounds through thiol-ene "click" reactions, yielding anionic, cationic, and zwitterionic self-assembled nanoparticles, respectively, in corresponding buffers. Polymeric nanoparticles with various sizes and surface charges can be prepared by altering side chain functionalities and pHs of dispersing media. This strategy can be further applicable to a variety of polymeric scaffolds to develop potential platforms for new drug delivery systems.

REVIEW

Stimuli-Responsive Graphene Oxide-Polymer Nanocomposites

Qi Lu, Hyo Seon Jang,
Wen Jiao Han, Jin Hyun Lee*,
and Hyoung Jin Choi*

Macromol. Res., **27**, 1061 (2019)

Graphene oxide (GO) as a high-performance stimuli-responsive ‘smart’ material has become a subject of great scientific value of its strongly hydrophilic behavior. GO based polymer nanocomposites have thus created a new class of polymer nanocomposites. This paper reviews their research progress. We focus on the GO based polymer nanocomposites with several stimuli responses by electric and magnetic fields, thermal, light, mechanical and pH input.

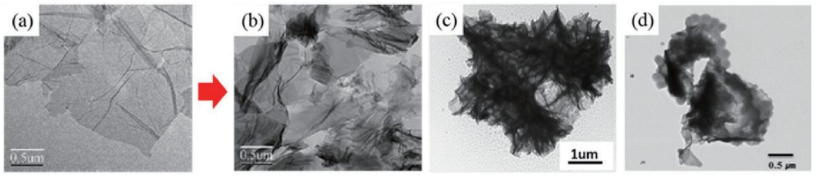

ARTICLES

Cationic Oligopeptide-Functionalized Mitochondria Targeting Sequence Show Mitochondria Targeting and Anticancer Activity

Yoonhee Bae, Chanyang Joo, Goo-Young Kim, Kyung Soo Ko, Kang Moo Huh, Jin Han*, and Joon Sig Choi*

Macromol. Res., **27**, 1071 (2019)

We demonstrated that mitochondria targeting sequence (MTS)-H_3R_9 peptide showed increased proton buffering effect and enhanced mitochondria-targeting efficiency compared to unmodified MTS peptide. We propose that the dual effect of MTS-H_3R_9 as a drug delivery vehicle and an anticancer reagent demands further studies ultimately aiming of developing novel combinatorial therapy for mitochondria-related diseases.

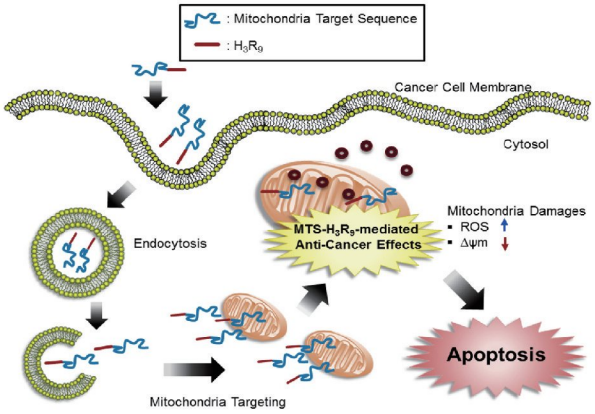

Cytotoxicity and *In Vivo* Biosafety Studies of the Poly(alkylphenol) Derivatives as Vulcanizing Agents

Yoon Ju Song, Joon Woo Chon, Hyuk Yoo, Jin Hwan Kim, and Dong June Chung*

Macromol. Res., **27**, 1081 (2019)

We investigated mechanical properties of rubbers with two different organic vulcanized agents derived from poly(alkylphenol) disulfide and their in vitro cytotoxicity and *in vivo* biological safety. Every compounded rubber sample containing poly(alkylphenol) disulfide vulcanizing agent showed not only improved elongation properties compared with the inorganic vulcanizing agent, but also good biocompatibility.

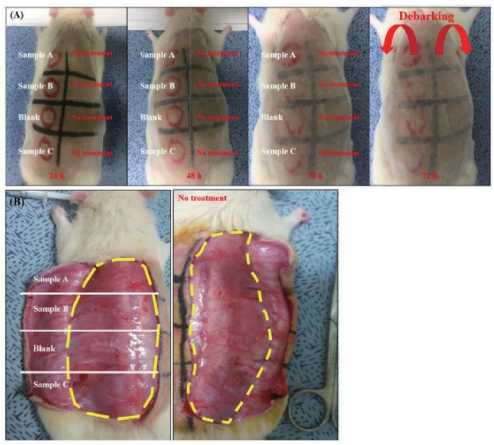

Magnetic Molecularly Imprinted Polymer Particles Based Micro-Solid Phase Extraction for the Determination of 4-Nitrophenol in Lake Water

Aziguli Yigaimu, Turghun Muhammad*, Wenwu Yang, Imran Muhammad, Muyasier Wubulikasimu, and Sergey A. Piletsky

Macromol. Res., **27**, 1089 (2019)

Preparation of a novel magnetic molecularly imprinted polymer (MMIP) for 4-nitrophenol (4-NP). The high selective material for 4-NP. Development of a dispersive solid-phase extraction method for 4-NP. Simple and green extraction with high recovery.

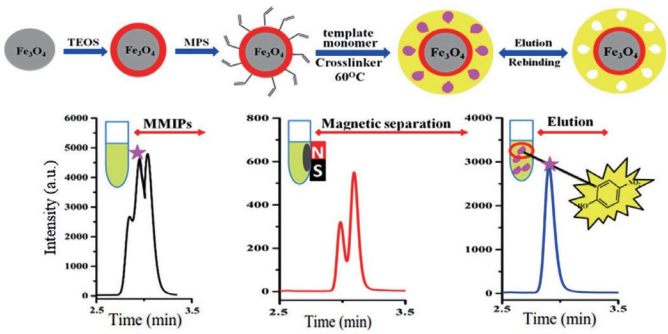

Biopeptide Hyperbranched Polyether Assembled from Lactic Acid, Glutamic Acid and Polyethylene Glycol Block Chains for Drug Loading

Linya Zhang*, Wei Xue, and Limin Gu

Macromol. Res., **27**, 1095 (2019)

A drug loading system is based on biopeptide hyperbranched polyether (BHPE). The biopeptide hyperbranched polymer (BHP) is composed of trimellitic anhydride, lactic acid and glutamic acid chains, and the BHPE is assembled by the BHP and polyethylene glycol 400 (PEG400).The SA-loaded BHPE system possess obvious core-skin structure, and it demonstrates good *in vitro* released performance.

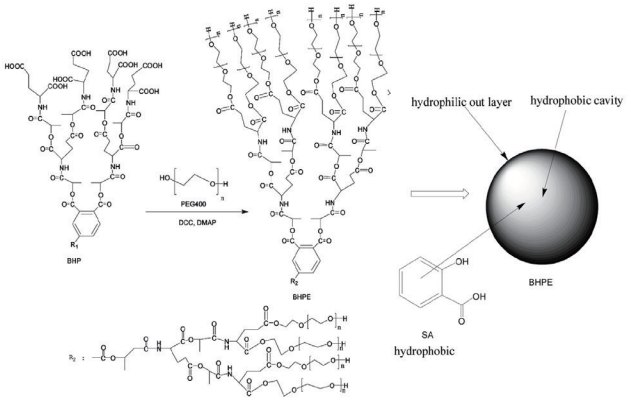

Facile and Affordable Process to Control Shell Thickness of Polydopamine-Assisted Polystyrene/Silver Core-Shell Particles

Jun Young Kim, Sung Ho Choi, Ji Hun An, and Seong Jae Lee*

Macromol. Res., **27**, 1104 (2019)

We prepared polystyrene (PS)/silver (Ag) core-shell particles with excellent electrical conductivity in a facile, affordable and eco-friendly way. The effect of glucose concentration on Ag shell thickness of polydopamine (PDA)-assisted PS/Ag core-shell particles was investigated. Thick and uniform Ag shell layer could be plated on PDA-coated PS particles, which rendered excellent electrical conductivity.

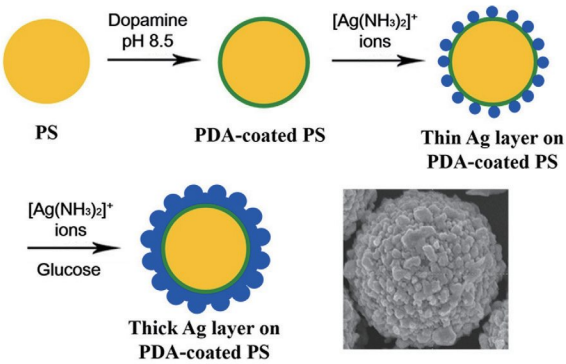

3-Arm PEG Based Amphiphilic Polymer Sorbents for Polar and Non-Polar Liquids

Soner Kizil and Hayal Bulbul Sonmez*

Macromol. Res., **27**, 1110 (2019)

Novel amphiphilic polymer sorbents consisting of glycerol ethoxylate and different organosilane crosslinker were fabricated. Synthesized star PEG based amphiphilic polymer sorbents have high affinity for water and organic liquids due to their hydrophobic and hydrophilic polymeric structure. Thus, the obtained polymeric networks behave as an organogel in oil medium, while they exist as a hydrogel in aqueous medium.

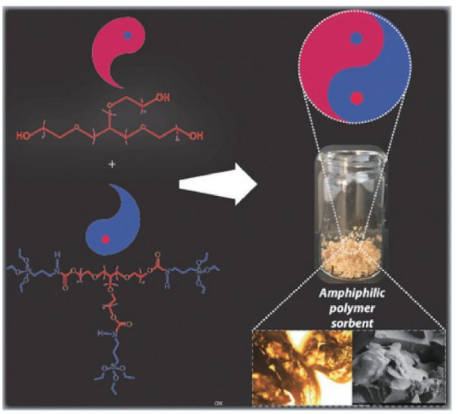

Enhancement of Thermal Conductivity of Poly(methylmethacrylate) Composites at Low Loading of Copper Nanowires

Nhat Anh Thi Thieu, Minh Canh Vu, Eui Sung Lee, Vu Chi Doan, and Sung-Ryong Kim*

Macromol. Res., **27**, 1117 (2019)

The exceptionally long copper nanowires (CuNWs) with high aspect ratios were synthesized by the chemical reduction method and incorporated into the poly(methylmethacrylate) (PMMA) matrix to fabricate thermally conductive PMMA composites. The thermal conductivity of PMMAcomposites reached the highest value of 0.85 W/mK at 2.0 wt% of CuNW loading, which corresponds to an enhancement of more than 400% compared to that of the neat PMMA. The significant improvement of thermal conductivity is attributed to the well-dispersed CuNWs in the PMMA matrix and the high aspect ratio of CuNWs. The experimental results of thermal conductivity fitted well with the Agari model.

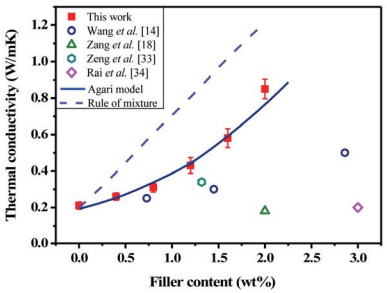

Reconstituted Fibril from Heterogenic Collagens-A New Method to Regulate Properties of Collagen Gels

Jian Yang, Haibo Wang*, Lang He*, Benmei Wei, Chengzhi Xu, Yuling Xu, Juntao Zhang, and Sheng Li

Macromol. Res., **27**, 1124 (2019)

Collagen molecules of heterogenic collagens could co-assemble in a way of quarter staggered arrangement to form novel collagen fibrils from the perspective of molecular level, whose structure and gel properties could be modulated by the species and ratio of the two collagens in heterogenic collagen reconstitution method, thus broadening the applications of the collagen-based materials.

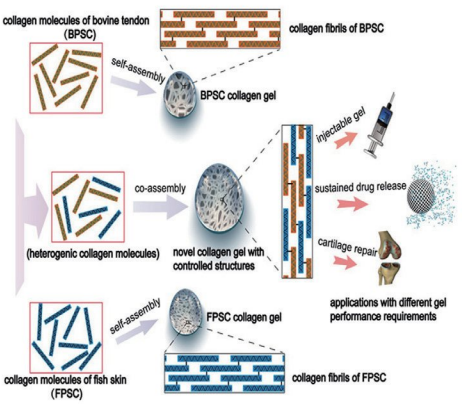

Improving Mechanical Properties and Thermal Conductivity of Styrene-Butadiene Rubber *via* Enhancing Interfacial Interaction Between Rubber and Graphene Oxide/Carbon Nanotubes Hybrid

Zhenghua Qian, Jianan Song, Zijin Liu, and Zonglin Peng*

Macromol. Res., **27**, 1136 (2019)

Graphene oxide (GO) was used to promote the dispersion of carboxylated multi-walled carbon nanotubes (CC) in the rubber matrix. π-π interactions and hydrogen bonds were constructed between GO and CC to obtain stable GO/CC hybrids. Carboxylated acrylonitrile butadiene rubber (xNBR) was used to enhance the interfacial interaction between the styrene-butadiene rubber (SBR) and the GO/CC hybrid. The carboxyl groups of xNBR could form hydrogen bonds with the oxygenated functional groups of GO/CC hybrid, and the backbone of xNBR could be crosslinked to SBR. As a result, mechanical properties and the thermal conductivity of SBR were significantly improved.

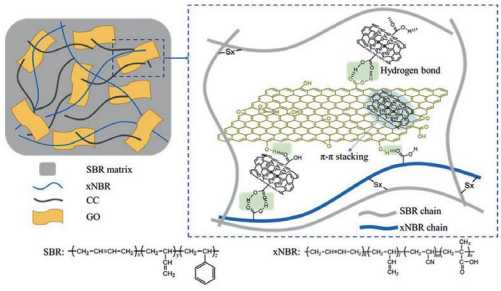

PVA Hydrogel Functionalization *via* PET-RAFT Grafting with Glycidyl Methacrylate and Immobilization with 2-Hydroxypropyltrimethyl Ammonium Chloride Chitosan *via* Ring-Open Reaction

Jinsheng Zhou*, Yanming Lin, Lin Ye, Ling Wang, Li Zhou, Huiyuan Hu, Qilong Zhang, Hui Yang, and Zhongkuan Luo*

Macromol. Res., **27**, 1144 (2019)

Polyvinyl alcohol (PVA) hydrogel has widely applied in biological industries, but it still faced the biofouling problem. To solve the biofouling problem, photoinduced electron transfer-reversible addition fragmentation chain transfer (PET-RAFT) polymerization and ring-open reaction were used in this work, and glycidyl methacrylate (GMA) and 2-hydroxypropyltrimethyl ammonium chloride chitosan (HACC) were grafted on the surface of PVA. After grafting, the properties of PVA were changed, especially the antifouling property. Due to the steric repulsion effect and surface hydration effect.

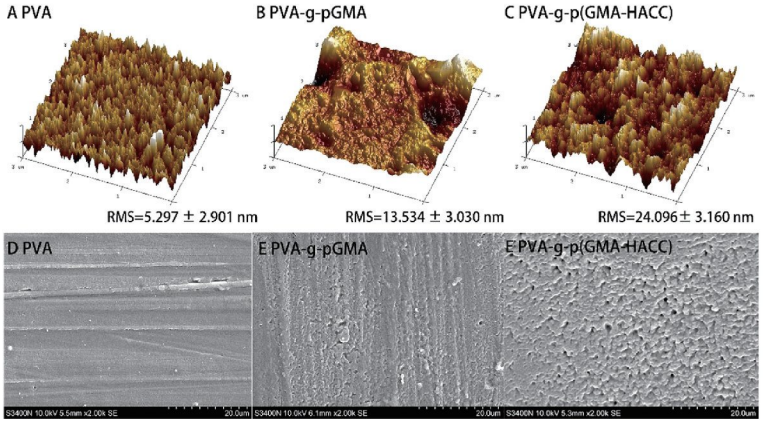

Autoclave Mediated Synthesis of Silver Nanoparticles Using Aqueous Extract of *Canna indica L.* Rhizome and Evaluation of Its Antimicrobial Activity

Narayanasamy Tamil Selvi, Rangaswamy Navamathavan, Hak Yong Kim*, and Rajkumar Nirmala*

Macromol. Res., **27**, 1155 (2019)

Autoclave mediated synthesis of silver nanoparticles by using aqueous rhizome extract of *Canna indica Linn* is reported. A fixed ratio of plant extract to metal salt was prepared and the mixture was allowed to autoclave for 15 min. The colour change was observed as red wine which evidenced the formation of silver nanoparticles. The silver nanoparticles were witnessed for antimicrobial activity against selected bacterial strains.

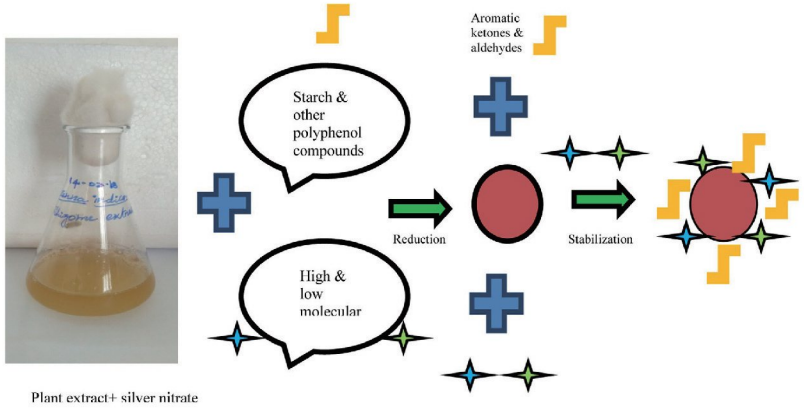

High-Performance Fluorinated Ethylene-Propylene/Graphite Composites Interconnected with Single-Walled Carbon Nanotubes

Ho-Joon Park, Jong Seok Woo, Sang Ha Kim, Kwang Sang Park, Sung Hoon Park, and Soo-Young Park*

Macromol. Res., **27**, 1161 (2019)

A novel method is described for the fabrication of highly conductive and flexurally strong fluorinated ethylene-propylene (FEP)/graphite nanocomposites by incorporating well-dispersed single-walled carbon nanotubes (SWCNTs) in the FEP matrix. The developed nanocomposites can potentially be used to prepare high-temperature bipolar plates for phosphoric acid fuel cells and heat-sink parts for vehicles.

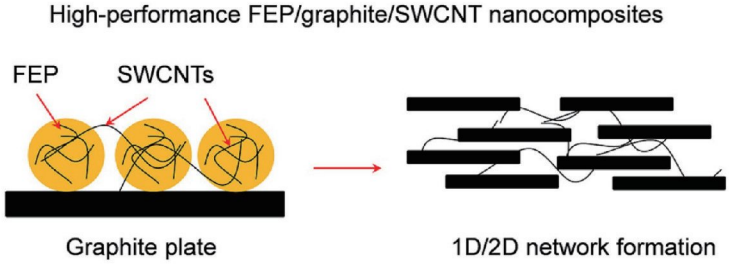

Intense Pulsed Light Sintered Core-Shell Nanoparticles for Organic Photovoltaic Devices

Soo Jung Yim, Ji Yeon Lee,
and Jae-Woong Yu*

Macromol. Res., **27**, 1167 (2019)

A high-speed and low-cost fabrication process using intense pulsed light sintering of metal nanoparticles was studied. Silver, copper, and four different alloy composition of copper-silver core-shell type nanoparticles were synthesized. The power conversion efficiency (PCE) and lifetime of the organic photovoltaic (OPV) fabricated with sintered metal electrode were studied. The device performance of OPV can be maintained with the copper to silver alloy ratio of 2. The use of metal alloy electrode could reduce the price of the silver electrode down 33%.

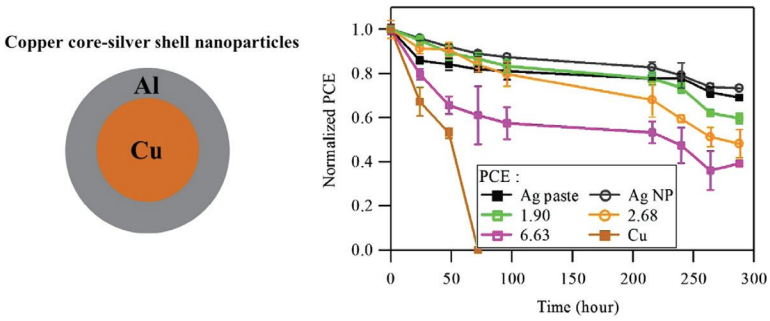

Preparation of Degradable Polymeric Nanoparticles with Various Sizes and Surface Charges from Polycarbonate Block Copolymers

Gyu Seong Heo, Sangho Cho*,
and Karen L. Wooley*

Macromol. Res., **27**, 1173 (2019)

Cover Paper

ABA-type block copolymers with pendant vinyl ether and benzyl ester functionalities were developed by organobase-catalyzed ring-opening polymerization of aliphatic cyclic carbonate monomers. The vinyl ether moieties on the resulting block copolymers were readily conjugated with 3-mercaptopropionic acid, cysteamine hydrochloride, and L-cysteine hydrochloride monohydrate through thiol-ene "click" reactions, yielding anionic, cationic, and zwitterionic nanoparticles, respectively.

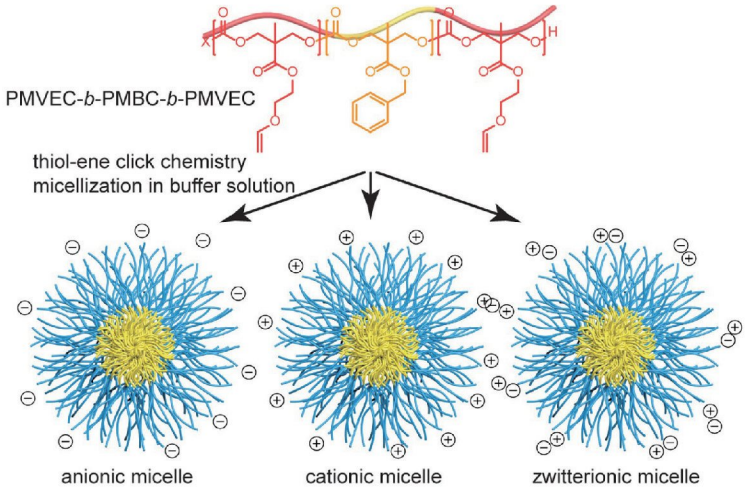

「Macromolecular Research」 목차

정기간행영문지_ 27권 12호 · 2019년 12월

COVER PAPER

Synthesis of Quinoxaline-Based Small Molecules Possessing Multiple Electron-Withdrawing Moieties for Photovoltaic Applications

Jun Tae Kim, Ho Cheol Jin, Sella Kurnia Putri, Dong Ryeol Whang, Joo Hyun Kim*, and Dong Wook Chang*

Vol. 27, No. 12, pp 1268-1274 (2019) | DEC 25, 2019 | DOI 10.1007/s13233-020-8002-7

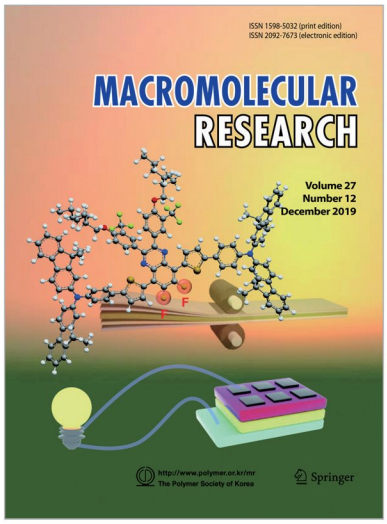

Owing to the significant contribution of the electron-withdrawing trifluoromethyl (CF_3) and fluorine (F) units, all inverted type organic solar cells based on conjugated small molecules exhibited high open circuit voltages greater than 0.82 V. In addition, the power conversion efficiencies (PCEs) of the devices were gradually improved with increasing number of fluorine atoms. The highest PCE (2.82%) with a open circuit volatge of 0.88 V, a short-circuit current of 6.38 mA cm^{-2}, and a fill factor of 50.6% was achieved.

ARTICLES

Curcumin Encapsulated Micellar Nanoplatform for Blue Light Emitting Diode Induced Apoptosis as a New Class of Cancer Therapy

Berwin Singh Swami Vetha, Eun-Mi Kim, Phil-Sun Oh, Suhn Hee Kim, Seok Tae Lim, Myung-Hee Sohn, and Hwan-Jeong Jeong*

Macromol. Res., **27**, 1179 (2019)

Blue light emitting diode (BLED) were known to inhibit cancer proliferation and induced apoptotic cell death by increasing intracellular reactive oxygen species (ROS) and caspase activation. However, not many attempts were made to study the naturally occurring photosensitizer molecule (PS) curcuminoids (CUR) mediated blue light emitting diode induced photodynamic therapy (BLED-PDT). Here, we demonstrated the use of pluronic F127 nanoplatform as a novel BLED-PDT based system for anticancer therapy. Aqueous soluble F127-CUR was proven to significantly mediate BLED-PDT, we anticipate that F127-CUR combined with BLED to induce BLED-PDT could be a promising cancer treatment modality.

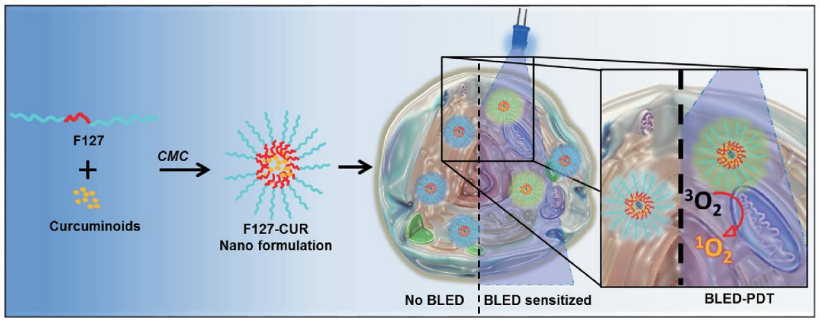

Effective Phosphorus/Phosphorus-Nitrogen Fire Retardants Applied to Biocomposites Based on Polypropylene-Wood Flour: Flammability, Thermal Behavior, and Mechanical Properties

Lam H Pham, Linh T Pham,
DongQuy Hoang*, and Jinhwan Kim*

Macromol. Res., **27**, 1185 (2019)

By adding diammonium phosphate (DAP) or aluminum diethyl phosphinate (OP) as flame retardants, flame retardancy of composites based on polypropylene and wood flour (PP-WF) improved significantly. A loading of 25 wt% DAP achieved a UL-94 V-0 rating as well as LOI value of 29%, which increased by 52.6% compared with that of the PP-WF composite alone. A 30 wt% OP loading provided a rating of UL-94 HB standard, and achieved LOI value of 28%. Meanwhile, the PP-WF composite without flame retardant, completely burned to the sample holder clamp with low LOI value (19%). Thermal properties of the PP-WF composite with and without DAP and OP flame retardants, were investigated using TGA and DSC. Flame retardant performance was also studied, through the morphology and chemical structure of residual char by TGA, FTIR, SEM, and XPS analyses. There was interaction between DAP and the composite, which played a key role in maintaining mechanical properties of the material.

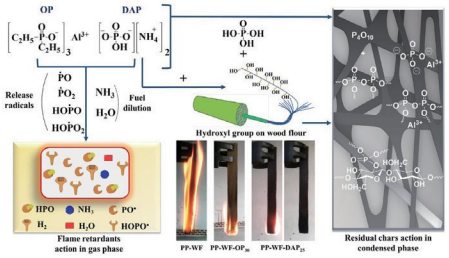

pH-Induced Crosslinking of Rice Starch *via* Schiff Base Formation

Narudom Srisawang,
Saksit Nobsathian,
Supa Wirasate,
and Chayanisa Chitichotpanya*

Macromol. Res., **27**, 1193 (2019)

The first synthesis of pH-induced crosslinking of rice starch without the use of any external chemical crosslinking agent is reported. It was prepared by forming the Schiff base (or imine) between the two modified starches: the oxidized rice starch and the amino rice starch. A pH-induced crosslinking reaction was demonstrated in which the crosslinking occurred under acidic conditions, whereas the hydrolysis occurred under basic conditions.

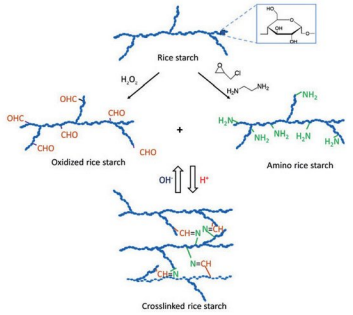

Molecular Dynamics (MD) Simulation of Zwitterion-Functionalized PMMA with Hydrophilic and Antifouling Surface Characteristics

Pedram Vousoughi,
Mohammad Reza Moghbeli*,
and Sousa Javan Nikkhah

Macromol. Res., **27**, 1200 (2019)

The simulation results showed a change in the behavior of the poly(methyl methacrylate) (PMMA) model, which was functionalized by the various amounts of the zwitterionic groups. The surface hydrophilicity increased with increasing the number of the zwitterionic groups. Further increase in the zwitterion level up to 16 wt%, (PMMA-Z16), caused difficulties in the reorientation of the functional groups and hydrophilic surface improvement. Functionalized PMMA model with 10 wt%, (PMMA-Z10), exhibited a proper modified PMMA structure with higher surface hydrophilicity and antifouling characteristics.

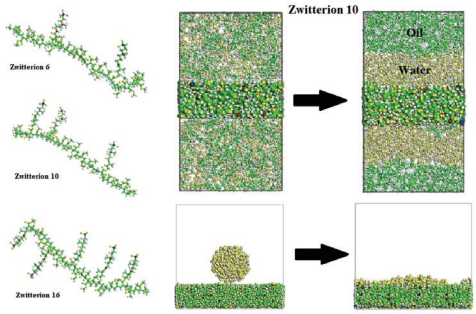

Correlation Between Shear-Flow Rheology and Solution Spreading During Spin Coating of Polysilane Solutions

Andreea Irina Barzic*,
Marius Soroceanu,
Raluca Marinica Albu,
Emil Ghiocel Ioanid,
Liviu Sacarescu, and Valeria Harabagiu

Macromol. Res., **27**, 1210 (2019)

The nature of polysilane substituent, affects its rheological behavior in toluene. Molecular modeling showed conformation in solution and polymer-solvent interaction. Flow behavior, spin speed, and spin time affect radial uniformity of wet film thickness. Polysilane solution adhesion to various substrates is evaluated.

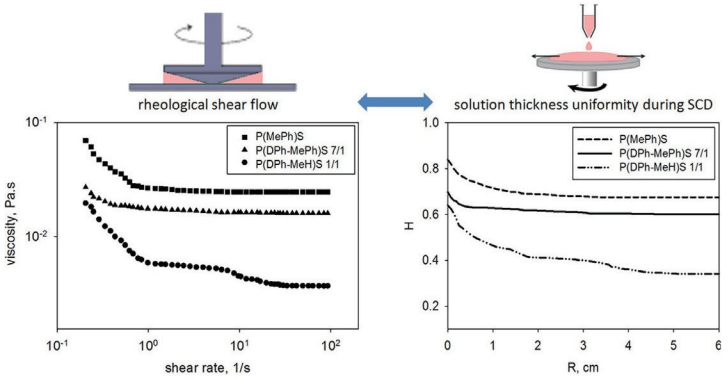

Effect of the Monomer Ratio on the Properties of Melt-Polymerized Polycarbonate

Byung Hoon Lim, Jin Woo Yi,
and O Ok Park*

Macromol. Res., **27**, 1221 (2019)

Hydroxide value as a function of the bisphenol A (BPA) residue from the actual data and data predicted by the Flory equation are plotted. The OH content and BPA residual amount are proportional. However the actual value tends to be slightly different from the value predicted by the Flory equation. In the Flory equation, the residual amount of BPA is less than 50 ppm at an OH content of less than 20%. In the actual data, the BPA content is less than 50 ppm at an OH content of less than or equal to 29%. For a product with a molecular weight of 10,500, the excess diphenyl carbonate (DPC) amount should be at least 3% relative to BPA, and it can be predicted more easily by the measurement of the OH content.

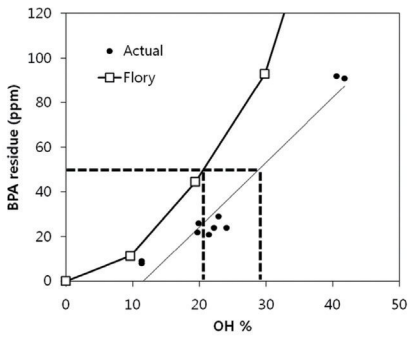

New One Step Self-assembly Strategy of Large-Area Highly Ordered, Crack-Free 2D Inverse Opal Films of Transition Metal Oxides and Its Application to Fabrication of Bilayer Inverse Opal Films

Hua Li*, Jian-feng Wang,
Jacques Robichaud, and Yahia Djaoued*

Macromol. Res., **27**, 1229 (2019)

Large area polystyrene (PS)/tungsten oxide (WO_3) and PS/titanium dioxide (TiO_2) opal composite monolayer films were generated using self-assembled polymeric colloidal spheres floating on aqueous WO_3 and TiO_2 precursors and were then used as building blocks to obtain highly ordered bilayer inverse opal (IO) films with homo- and hetero-structure *via* repeated operations of this one step self-assembly method.

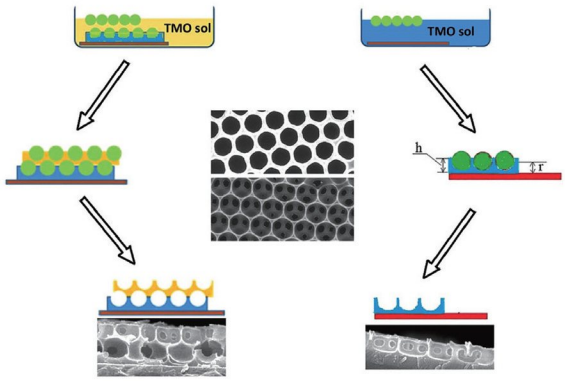

Sulfonated Cross-Linked Poly(ether ether ketone) Films with Wrinkled Structures: Preparation and Vanadium Ions Permeability

Abdul G. Al Lafi*, Reem Hasan, and Nedal Al-Kafri

Macromol. Res., **27**, 1239 (2019)

Sulfonation of ion irradiated poly(ether ether ketone) introduced a variety of wrinkling patterns on the surface of membranes. The wrinkles were controlled by varying the degree of sulfonation, cross-linking density and ion irradiation conditions. The membranes produced are promising for applications that require large-surface area and uniform surface patterning. They had a low permeability of vanadium ions, *i.e.* 1.5×10^{-7} cm^2 min^{-1}.

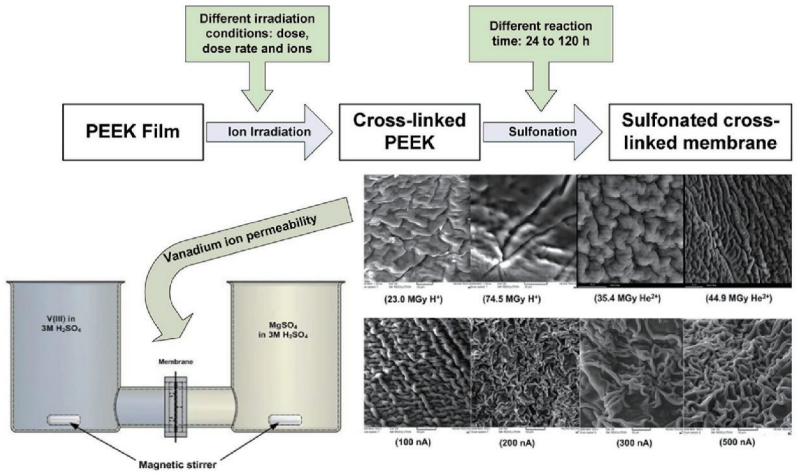

All-Benzocyclobutene Functionalized Polycarbosilane and Derived Copolymers with Low Dielectric Constant and High Thermal Stability

Nan Zhong, Xian Li, Huan Hu, Yawen Huang, Xu Ye*, and Junxiao Yang*

Macromol. Res., **27**, 1248 (2019)

All-benzocyclobutene functionalized polycarbosilane was prepared by ring-opening polymerization. The derived cured resin has a low-dielectric constant (2.42), high thermal stability ($T_{5\%}$ = 506 °C) and high modulus (6.3 GPa).

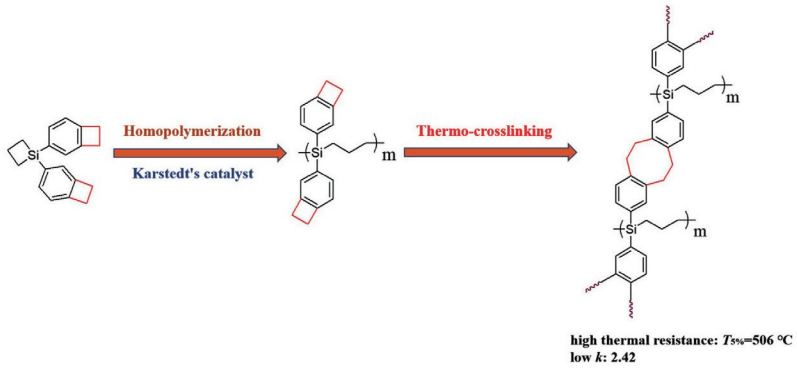

Sequential Symmetry-Breaking Intercolumnar Transformations of a Conjugated Rod Molecule with a Flexible Coil

Young-Min Lee, Ho-Joong Kim, and Byoung-Ki Cho*

Macromol. Res., **27**, 1255 (2019)

Penta-*para*-phenylene rod linked to a poly(ethylene oxide) coil exhibited sequential intercolumnar transformations from *c2mm* to *p2gg* to *p6mm* symmetry with increasing temperature. The observed symmetry-breaking transitions occurred *via* the thermally-induced rotation of the ribbon-like aromatic columns along the columnar axis, which was not accompanied by enthalpy change.

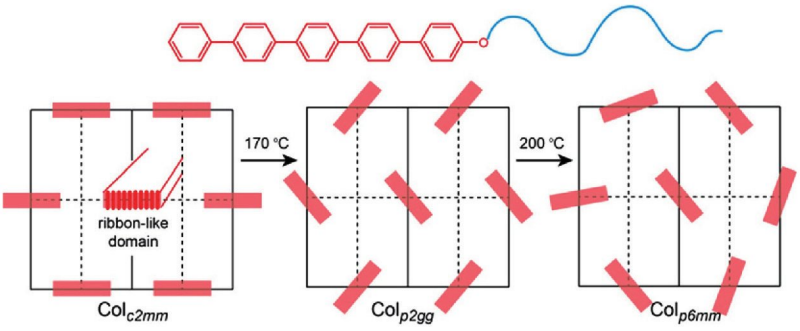

Synthesis and Characterization of Benzothiadiazole and Dicyanovinylindandione Based Small-Molecular Conjugated Materials and Their Photovoltaic Properties

Ratna Dewi Maduwu, Ho Cheol Jin, and Joo Hyun Kim*

Macromol. Res., **27**, 1261 (2019)

A series of non-fullerene small molecules (**BT-T-IDC** and **BT-T-tB-IDC**) with the architecture of A1-π-A2-π-A1 (acceptor 1-π-acceptor 2-π-acceptor 1), have been synthesized. The device based on **BT-T-tB-IDC** showed a better PCE.

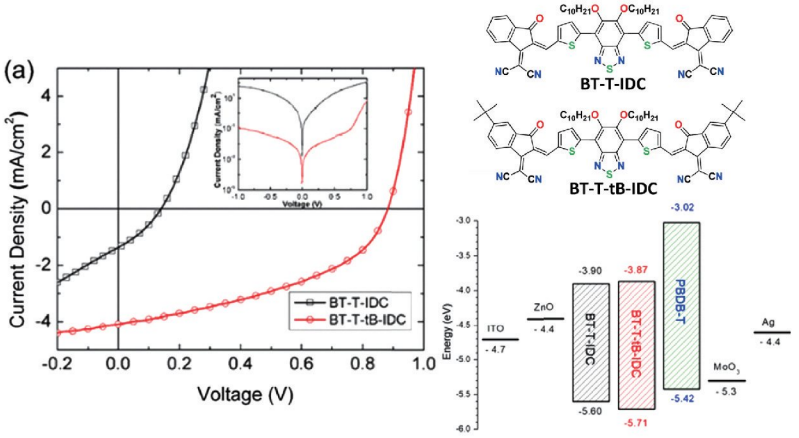

Synthesis of Quinoxaline-Based Small Molecules Possessing Multiple Electron-Withdrawing Moieties for Photovoltaic Applications

Jun Tae Kim, Ho Cheol Jin, Sella Kurnia Putri, Dong Ryeol Whang, Joo Hyun Kim*, and Dong Wook Chang*

Macromol. Res., **27**, 1268 (2019)

Cover Paper

Three quinoxaline-based small molecules possessing multiple electron-withdrawing moieties were synthesized. The electron-donating triarylamine units were linked to both ends of electron-accepting 2,3-diphenyl quinoxaline (DPQ) derivatives with strong electron-withdrawing trifluoromethyl (CF_3) moieties. Owing to the significant contribution of the electron-withdrawing CF_3 and fluorine units, the highest PCE (2.82%) with a V_{oc} of 0.88 V, a short-circuit current of 6.38 mA cm^{-2}, and a fill factor of 50.6% was achieved achieved from the device based on **CF3Qx-2F**.